JOURNAL OF CATALYSIS 132, 319–342 (1991)

Phase Cooperation between Tin and Antimony Oxides in Selective Oxidation of Isobutene to Methacrolein

I. Mechanical Mixtures of SnO_2 and α-Sb_2O_4

L. T. WENG, N. SPITAELS, B. YASSE, J. LADRIÈRE,* P. RUIZ, AND B. DELMON[1]

*Unité de Catalyse et Chimie des Matériaux Divisés and *Unité de Chimie Inorganique et Nucléaire, Université Catholique de Louvain, Place Croix du Sud 1, 1348 Louvain-la-Neuve, Belgium*

Received March 26, 1990; revised February 26, 1991

Results are reported concerning the cooperation between SnO_2 and α-Sb_2O_4 particles in the selective oxidation of isobutene to methacrolein. The catalysts were prepared by mechanically mixing the corresponding powders. A conspicuous catalytic synergy was observed when methacrolein production and selectivity to methacrolein formation were considered. The catalysts, both fresh and used, were characterized by XRD, ^{119}Sn Mössbauer spectroscopy, XPS, analytical electron microscopy (AEM), and ESR in order to investigate the origin of the synergy observed. The joint use of these techniques yielded no indication that a new phase (or solid solution) formed or that mutual surface contamination during either the preparation of the mixture or the catalytic test took place. Within the sensitivity limits of the techniques used, the mechanical mixtures can be considered as composed of two pure separate phases in good contact. The origin of the observed synergy and the other experimental observations is explained in a satisfactory manner by the existence of a "remote control" mechanism, i.e., that α-Sb_2O_4 produces a mobile oxygen species, namely spillover oxygen, which, by flowing onto the surface of SnO_2, creates on the surface of the latter new selective sites and/or regenerates those which have become deactivated. Spillover oxygen produced by α-Sb_2O_4 seems to control the selective catalytic sites on SnO_2 by inhibiting their transformation to reduced, nonselective sites. Spillover oxygen also inhibits the formation of carbonaceous deposits.

INTRODUCTION

Since the discovery of the Sohio catalysts (bismuth molybdates) for the production of acrylonitrile (*1*), many fundamental studies have been conducted to elucidate the mechanism of the catalytic process. The majority of these studies were concerned with single-phase systems, particularly those comprised of oxides of complex composition (oxides of more than one single element) with defined structures, such as molybdates (Bi_2MoO_6, etc.) or antimonates (USb_3O_{10}, etc.). By comparison, very little research has been devoted to the study of multiphase catalysts, although most industrial catalysts are comprised of more than one phase. One reason for this may be the difficulties encountered in distinguishing the relative contribution of each phase to the overall behavior of composite catalysts. Another reason for focusing attention on single-phase catalysts is the difficulty encountered in characterization of more complex solids. For a long time, no evidence existed to show that the mechanism of the reaction might demand the presence of two or several phases. It was indeed reasonable to consider that an industrial catalyst containing many elements possessed a single active phase (i.e., an adequately doped compound oxide). If this point of view were adopted, the other phases present in the catalyst could be thought to be necessary for adjusting prop-

[1] To whom correspondence should be addressed.

0021-9517/91 $3.00

TABLE 1

Examples of Multiphase Catalysts Used in Selective Oxidation (from Refs. (*2—19*))

System	Reaction	Refs.
Sb_2O_4—MoO_3	Isobutene → methacrolein	(*2*)
SnO_2—MoO_3	Sec-butyl-alcohol → methyl-ethyl-acetone	(*3, 4*)
Sb_2O_4—$Sn(Sb)O_2$		
Sb_2O_4—SnO_2	Propylene → acrolein	(*5*)
Sb_6O_{13}—SnO_2		
β-$CoMoO_4$—$Fe_2(MoO_4)_3$—Bi_2MoO_6	Butene → butadiene	(*6*)
$MgMoO_4$—$Fe_2(MoO_4)_3$—$Bi_3(FeO_4)(MoO_4)_2$	Propylene → acrolein	(*7*)
$Bi_2Mo_3O_{12}$—MoO_3—$CoMoO_4$	Propylene → acrolein	(*8*)
$NiMoO_4$—MoO_3	C_4 → maleic anhydride	(*9*)
$CoMoO_4$—MoO_3	Propylene → acrolein	(*10*)
$MgMoO_4$—MoO_3	Propylene → acrolein	(*11*)
$Fe_2(MoO_4)_3$—MoO_3	Methanol → formaldehyde	(*12*)
UO_2MoO_4—MoO_3	Isobutene → methacrolein	(*13*)
$Bi_2Mo_3O_{12}$—$Ce_2Mo_3O_{12}$	Propylene → acrolein	(*14*)
$FeSbO_4$—Sb_2O_4	Propylene → acrolein	(*15, 16*)
Bi_2MoO_6—$Bi_2Mo_3O_{12}$	Propylene → acrolein	(*17*)
$ZnFe_2O_4$—Fe_2O_3	Butene → butadiene	(*18*)
$MgFe_2O_4$—Fe_2O_3	Butene → butadiene	(*19*)

erties like mechanical strength and resistance to sintering, but not to play a direct role in the catalytic process.

There is now incentive to study multiphase catalysts. Modern physico-chemical techniques allow for a more detailed description of the structure and texture of complicated catalysts. Some studies (*2–19*) dealing with multiphase catalysts have been published (Table 1). The results show that multiphase catalysts are often more active and selective than single phases. Several different explanations for the observed synergy between phases have been proposed, some of them contradictory.

A series of investigations on the synergy between separate phases has been conducted in our laboratory in recent years. Our previous research program was devoted to the synergy between oxides in *N*-ethyl formamide dehydration (*20, 21*). This reaction constitutes a very good model because the synergy observed between phases cannot be interpreted by a bifunctional catalytic mechanism. Molecular oxygen is not involved directly in the dehydration process but is indispensable for maintaining the catalyst active and selective. It has also been noted that the catalysts active and selective in this reaction are identical in composition to the oxide catalysts exhibiting high activity and selectivity in selective oxidation (Bi–P–Mo, Bi–Mo, Sb–Mo, Sb–Sn, etc.). In particular, it has been shown that there is a synergy between MoO_3 and $BiPO_4$ (*20*) and MoO_3 and Sb_2O_4 (*21*). This synergy exists even when the starting oxides are brought together by a simple mechanical mixing in order to minimize mutual contamination and mechanical damage of the crystallites. The joint use of several physicochemical techniques showed that these mixtures were composed of the noncontaminated starting phases and that they remained unchanged after catalytic work. To account for these results, a new mechanism designated remote control has been proposed. This mechanism supposes that a mobile oxygen species (spillover oxygen) is formed from O_2 on one of the phases ($BiPO_4$ or

Sb_2O_4) and migrates onto the surface of the other (MoO_3), where it creates and/or regenerates the catalytic centers.

The surprising key role of oxygen in *N*-ethyl formamide dehydration, and the great similarity in composition between the corresponding catalysts and those active in selective catalytic oxidation led us to investigate whether a similar mechanism might play a role in the latter process. More specifically, the question was whether the same kind of synergy between oxides existed in selective oxidation and, if so, whether the same remote control mechanism could be operative. An initial study concerned MoO_3–Sb_2O_4 mixtures and their behavior in the selective oxidation of isobutene to methacrolein (*2*). It was observed that a conspicuous synergy did indeed exist. Numerous arguments led us to propose that a remote control mechanism could explain the observed effects.

The present study is part of a series of publications presenting the results observed with the SnO_2–Sb_2O_4 catalyst. The aim of this first part is to demonstrate the existence of a cooperation between separately prepared SnO_2 and Sb_2O_4 powders when mixed together, and to shed some light on the origin of this cooperation.

The single SnO_2 and Sb_2O_4 oxides were subjected to the same mechanical mixing procedures as in the previous studies. The reaction was the selective oxidation of isobutene to methacrolein,

$$CH_2{=}C(CH_3){-}CH_3 + O_2 \rightarrow CH_2{=}C(CH_3){-}CHO + H_2O,$$

an example of allylic oxidation. This oxidation is of practical interest, as it constitutes the first step of a route to producing MMA (methyl methacrylate).

Several processes can take place when two oxides are mixed together. Consequently there may exist different explanations for a synergy:

(1) formation of a new compound or a solid solution by reaction between two phases;

(2) contamination of the surface of one phase by elements coming from the other, namely mutual contamination, such as SnO_2 by Sb or vice versa (this is distinct from surface contamination by coke, which is discussed below);

(3) formation of a monolayer of one oxide over the other (a special form of contamination);

(4) classical bifunctional catalysis; and

(5) formation of mobile oxygen species and some chemical action of the latter.

In the last of these cases, two possibilities appear: (a) the mobile oxygen species produced from one phase react directly with reactants adsorbed on the other (spillover oxygen being used as a reactant) and (b) the mobile oxygen species emitted from one phase migrates onto the surface of the other and, by reacting with it, improves the catalytic activity (spillover oxygen being used as a controlling species)—this is the remote control mechanism.

In order to identify the real nature of the process occurring in these mechanical mixtures and to explain correctly the origin of the cooperation between phases, a very complete characterization with X-ray diffraction, ^{119}Sn Mössbauer spectroscopy, SEM, AEM (analytical electron microscopy, or electron probe microanalysis made inside a conventional electron microscope), XPS, and ESR had to be performed.

X-ray diffraction is usually used to detect the formation of new compounds. In the present case concerning SnO_2 and Sb_2O_4, in fact, very few reports (*22*) in the literature have proposed the existence of compound oxides between Sn and Sb. However, the formation of a solid solution between Sn and Sb oxides has often been considered, especially for catalysts prepared by coprecipitation (*23, 24*). Therefore, special attention should be paid to this point. If a solid solution, i.e., an oxide constituted of Sb^{5+},

dissolved in the SnO_2 lattice (as is usually proposed in the literature) is formed, it may be possible to observe a small change of the crystallographic parameters; this has been observed in Ref. (*25*) for coprecipitated catalysts and in Ref. (*26*) for impregnated catalysts. We used a very sensitive diffractometer to check this point. Another useful tool with which to detect the formation of solid solution is ^{119}Sn Mössbauer spectroscopy, since a higher isomer shift and quadrupole splitting were observed for solid solution (*23*). Moreover, it has been mentioned in the literature (*27*) that SnO_2 covered with a film of Sb_2O_4 exhibits a special ESR signal ($g = 1.8733$). This signal can be attributed to the formation of trapped electrons in the anionic oxygen vacancies, which result from the incorporation of Sb^{5+} into the SnO_2 lattice, i.e., from the formation of a solid solution of Sb^{5+} in SnO_2. Therefore, ESR was also used as a complementary tool to detect the formation of solid solutions such as Sb^{5+} in SnO_2.

Mutual surface contamination or monolayer formation can, in principle, be detected by means of AEM and XPS. AEM can yield information concerning the composition of each particle of each phase, while XPS can reveal the composition of the outermost surface layers of the sample.

Another means of clarifying the origin of cooperation is to investigate whether different experiments, e.g., solid state phenomena, or the experimental influence of reaction parameters on the catalytic behavior match the predictions made on the basis of a given mechanism. If spillover oxygen species migrate from one phase to another, it could be speculated that solid state oxidation–reduction phenomena would occur at different rates on one phase when mixed with the other phase. Along a different line of thought, several predictions can be made with respect to catalytic behavior, if the remote control mechanism operates in the SnO_2–Sb_2O_4 system. First, with oxygen species being involved in the remote control mechanism, it can be expected that the influence of oxygen concentration on catalytic behavior would be different when the phase that plays the role of donor of oxygen species (α-Sb_2O_4) is present or not. Second, the ratio between the surface areas developed by each phase would necessarily influence the cooperation, because the remote control mechanism involves two surface phenomena: (i) the formation of a mobile species on the surface of a phase and (ii) the reaction of this species with the surface of the other. Therefore, our experiments included variations of the oxygen concentration and the surface area of SnO_2 in order to check these predictions.

EXPERIMENTAL

Starting Materials

The products used as starting materials for catalyst preparation were tin(II) chloride, $SnCl_2 \cdot 2H_2O$, and antimony(III) oxide Sb_2O_3; all these were Merck p.a.

Gases were from L'Air Liquide (isobutene $\geq$ 99%, He 99.995%, H_2 99.9%, O_2 99.5%, and $N_2 \geq$ 99.8% and were used without any further purification.

Catalysts Preparation

Pure α-Sb_2O_4 (1.9 m^2/g) was obtained by calcination of Sb_2O_3 in air at 500°C for 20 h.

Two sources of pure SnO_2 were used, both prepared by precipitation as follows. $SnCl_2 \cdot 2H_2O$ was dissolved in water. A precipitate was formed after addition of NH_3 solution (28%, Union Chimique Belge). When the precipitation was complete (the final pH value was about 7.5), the precipitate was filtered and washed with an aqueous NH_3 solution, followed by drying at 110°C for 16 h. SnO_2(I) (12.6 m^2/g) and SnO_2(II) (5.4 m^2/g) were obtained by calcining this precipitate at 600°C for 8 h and 900°C for 16 h, respectively.

Mechanical mixtures were obtained by vigorously mixing the suspension of the powders in a light paraffin (*n*-pentane) for 10 min by means of a mixer (ultra-turrax from Janke & Kunkel). After evaporation of the solvent under reduced pressure, the mixtures so obtained were finally dried at

80°C overnight. No further calcination was carried out.

Powder mixtures of composition

$$R_m = \frac{SnO_2}{SnO_2 + \alpha\text{-}Sb_2O_4} \quad \text{(expressed as mass ratio)} \quad (1)$$

varying from 0 to 1 were prepared. Hereafter, the mechanical mixture is denoted as M_y^x, where x refers to the type of SnO_2 used (I or II) and y refers to the concentration (R_m) of SnO_2 in mechanical mixture. For instance, M_{50}^I is the mixture containing 50% SnO_2(I) and 50% α-Sb_2O_4.

Catalysts Characterization

The fresh and used catalysts were characterized by several different physico-chemical techniques.

BET. BET surface areas were measured gravimetrically in a Setaram MTB 10-8 microbalance connected to a vacuum and gas handling system using N_2 adsorption at 77 K.

X-ray diffraction. X-ray diffraction measurements were made in a Kristalloflex 805 Siemens diffractometer using a Ni-filtered Cu$K\alpha$ radiation. In order to check for the possible formation of a solid solution, a more sensitive diffractometer (Siemens D-500, again using the Cu$K\alpha$ radiation) was also used.

Electron microscopy. Electron microscopy and electron microanalysis (AEM) were performed with a Jeol Temscan 100 CX electron microscope equipped with a Kevex 5100 C energy dispersive spectrometer. The samples were ground, dispersed in a solvent (*n*-pentane), and deposited on a carbon film supported on a copper grid.

Samples were examined by means of conventional transmission (CTEM) and secondary electron (SEM) modes, which gave an overview of the morphological structure of the samples. The AEM analysis of different particles was carried out with an energy dispersive spectrometer.

In AEM, the analyzed thickness is usually that of the observed particles with an upper limit of about 1 μm if thick particles are used (with our samples of surface area 1.9, 5.4, and 12.6 m^2/g, individual particles have average dimensions less than 0.5 μm). Lateral resolution with thick particles is about 1 μm and becomes much better with thin particles (50 to 100 nm in our case). In principle, AEM permits the detection of a contaminant at the level of 1%. However, Sn and Sb are neighbors in the periodic table, and the last two L lines of Sn overlap with the first two L lines of Sb. As a consequence, only the first L line (strongest) of Sn and the third L line and the K lines of Sb can be used. This slightly decreases the detection sensitivity for Sb.

^{119}Sn Mössbauer spectroscopy. The ^{119}Sn Mössbauer measurements at room temperature were performed in the constant acceleration mode. The source was $Ca^{119}SnO_3$. Isomer shifts (IS) and quadrupole splitting (QS) were calculated and compared to pure SnO_2. Experimental errors for IS and QS were ± 0.05 mm/s.

ESR. Some ESR measurements were made with a X-band Varian-12 spectrometer equipped with two cavities, using a modulation of 100 kHz. The incident microwave beam powder was 20 mW. The sample holder was a small quartz tube, with a diameter of 4 mm. In each run, about 300 mg of sample was put into the sample holder (with 1.5 cm height in holder) and the spectrum was recorded at room temperature.

X-ray photoelectron spectroscopy. XPS measurements were performed in a Vacuum Generators ESCA-3, equipped with a Tractor Northern TN 170 accumulator allowing one to scan the same region several times in order to improve the signal/noise ratio. The excitation radiation was Mg$K\alpha$ (1253.6 eV). This machine is not equipped with a flood gun. With relatively insulating substances such as our samples, the surface charging effect impairs resolution. This effect is more evident for the mixtures of two oxides having very different conductivity. We could not separate with confidence the $Sb_{3d_{3/2}}$

peaks of Sb_2O_4 (539.6 eV for $Sb^{(III)}$; 540.1 eV for $Sb^{(V)}$ referenced to C_{1s} (284.6 eV)).

Sample powders were compressed in small cups, which were supported horizontally in a holding axle. Six samples fit simultaneously in the instrument, of which five were catalysts and one was SiO_2, which was used as an external reference. The C_{1s}, $Sb_{3d_{5/2}} + O_{1s} + Sb_{3d_{3/2}}$, $Sn_{3d_{5/2}} + Sn_{3d_{3/2}}$ signals were accumulated successively for each sample. The binding energy values were calculated with respect to contaminant carbon C_{1s} (BE = 284.6 eV). The concentrations were calculated from XPS intensities using

$$\frac{\mathbf{C}_A}{\mathbf{C}_B} = \frac{\mathbf{I}_A/\mathbf{f}_A}{\mathbf{I}_B/\mathbf{f}_B}, \qquad (2)$$

where $\mathbf{I}_A$, $\mathbf{I}_B$ are the normalized intensities measured by XPS while $\mathbf{f}_A$, $\mathbf{f}_B$ are the atomic sensitivity factors given by Wagner *et al.* (*28*).

In our case, because $Sb_{3d_{5/2}}$ was overlapped with O_{1s}, $Sb_{3d_{3/2}}$ and $Sn_{3d_{5/2}}$ were used to calculate the corresponding Sb and Sn concentrations. In the present case, no suitable internal reference can be employed (O_{1s} is not acceptable because of its overlapping with $Sb_{3d_{5/2}}$). The concentrations were calculated with respect to that of the external reference SiO_2 (C_{sb}/C_{Si}, C_{Sn}/C_{Si}).

The use of an external reference has two advantages. The first is to make easier the comparison of results obtained from different measurements, even if the measuring conditions change slightly. The second and main advantage appears when multiphase ($A + B$) catalysts are studied. One knows that the sintering of one phase, e.g., A would bring about a relative decrease of the signals of A; similarly, surface contamination of A by B would bring about a relative increase of the signal of B or a decrease of that of A. However, it is not always recognized that another cause for a decrease of the signal of A might exist, namely that A becomes selectively covered by an external contaminant: in our case, we see that selective coke deposition may indeed occur under certain conditions. The use of an external standard is very convenient and helpful for avoiding pitfalls in the interpretation. For example, all cases examined above bring about a change of the A/B signal ratio. In the first two cases, all intensities measured against an external standard change (decrease or, respectively, increase). When selective contamination occurs on A, the corresponding intensity decreases, but that of B remains constant. The use of an external standard may also allow a higher precision in the measurement of relative concentration at surfaces.

In a general way, in a mixture containing two phases, A and B, the surface composition measured by XPS can be affected by several factors. The difference in escape depth of the photoelectrons of Sb and Sn is very small

$$\lambda_{Sn_{3d_{5/2}}} = 1.18\ \text{nm}, \quad \lambda_{Sb_{3d_{3/2}}} = 1.22\ \text{nm}$$

because they correspond to similar binding energies, and the densities of Sb_2O_4 and SnO_2 are similar. Account being taken of that, the factors that may affect the surface composition, as measured by XPS, are

(i) the difference of particle size between two phases;

(ii) the aggregation of the particles of one phase;

(iii) the contamination of the surface of one phase by elements emanating from the other or monolayer formation;

(iv) the mutual arrangement of the particles of one species with respect to the other (covering one phase by particles of the other);

(v) specific deposition of an impurity (carbon, etc.) on one of the phases.

Therefore, special care should be taken when interpreting the XPS results.

In the present case, the particle size of SnO_2(I) is much smaller than that of Sb_2O_4 ($S_{SnO_2(I)} = 12.6\ m^2/g$, $S_{Sb_2O_4} = 1.9\ m^2/g$). If there is no self-aggregation of each oxide in the fresh mixtures, the surface accessible to

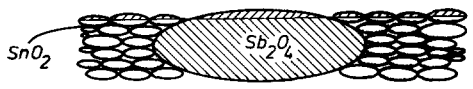

SCHEME 1. Schematic representation of surface accessible to XPS for SnO_2 and Sb_2O_4, respectively, in mechanical mixtures 50/50 SnO_2/Sb_2O_4 (the thin hatched layer on top represents the portions of the samples that emit photoelectrons to the detector).

XPS of SnO_2 should be higher than that of Sb_2O_4; i.e., we should observe an increase of the Sn signal with respect to bulk composition. This situation can be represented in Scheme 1, which illustrates, very schematically, the case of M^1_{50}.

This would, without doubt, complicate the interpretation of XPS results because the enrichment of Sn measured by XPS with respect to bulk composition may also result from the surface contamination of Sb_2O_4 by Sn. This possibility is schematized in Scheme 2.

The question is, How can we distinguish between these two possibilities? In fact, if the enrichment is due to surface contamination, i.e., if Sn covers Sb_2O_4, the increase of the Sb signal should always be observed, even if the particle size is modified. Conversely, if the difference in particle size is the cause of signal increase, the change of the particle size of either SnO_2 or Sb_2O_4 would alter the magnitude of this increase and this would disappear (or the surface composition measured by XPS would become rigorously proportional to bulk composition) when the particle sizes of SnO_2 and Sb_2O_4 are the same. The comparison of results obtained with the SnO_2(I)–Sb_2O_4 and the SnO_2(II)–Sb_2O_4 systems shows that the explanation is the second one.

The other difficulty in the present case is that the XPS signal of Sn is "masked" by the deposition of coke for the samples after reaction, as can be seen below. In this way, the surface composition measured by XPS would not reflect the extent of near surface zones emitting photoelectrons in the direction of the detector: deposited coke stops some photoelectrons and decreases the Sn XPS signal. The solution was to eliminate the coke by calcination of the samples containing coke in air at 400°C for 20 h.

Catalytic Activity Measurements

The selective oxidation of isobutene to methacrolein was carried out in a continuous gas-flow fixed-bed reactor system. The reactor consisted of a Pyrex U-tube of 8 mm internal diameter into which a small tube of 4 mm in external diameter was inserted for loading a thermocouple for temperature measurement in the catalytic bed (Scheme 3). The catalyst was packed in the central section of the reactor and the top (8 cm) and bottom (10 cm) sections were packed with glass pills of 1000 μm diameter. The height of the catalytic bed was about 1 cm (sometimes 0.5 cm: see below). In order to minimize the pressure drop, the catalysts were ground and sieved. The fractions between 500 and 800 μm were used. The composition and flow rate of the gas feed mixture were measured and controlled using mass flow controllers, which were calibrated for each of specific gases (isobutene, oxygen, and nitrogen).

The remaining reactants and the reaction products were passed through a gas-phase chromatography apparatus (Intersmat, IGC 120 ml) for analysis. The connection between the reactor and the chromatographic equipment was kept at 150°C in order to avoid any condensation. Two columns were employed, one containing Tenax for analyzing the methacrolein and the other oxygenated products (acrolein, alcohols) and the

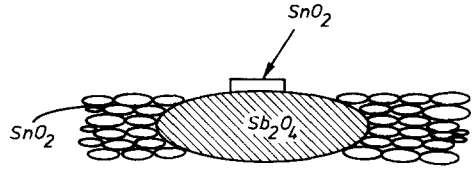

SCHEME 2. Schematic representation of surface contamination of Sb_2O_4 by SnO_2.

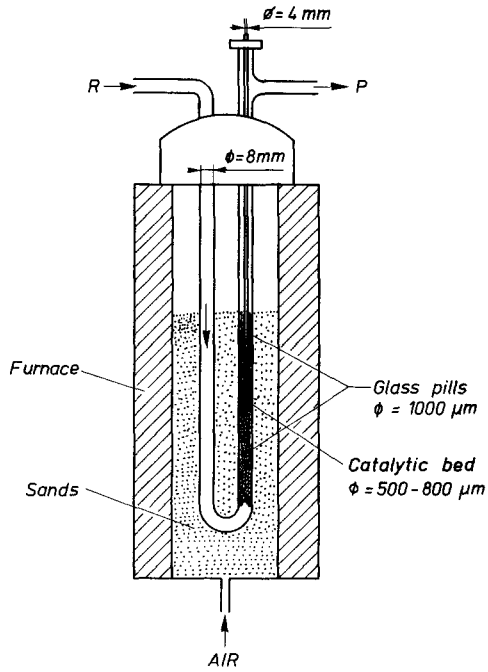

SCHEME 3. Catalytic reactor used in selective oxidation of isobutene.

other containing Porapak Q for isobutene, CO/CO_2, N_2, and water.

The standard reaction conditions were as follows: partial pressure of isobutene 76 mm Hg; partial pressure of oxygen 152 mm Hg; total pressure 760 mm Hg; total feed rate 30 ml/min; reaction temperature 380–420°C. We chose the weight of catalyst in order to satisfy the following conditions: (i) there should exist a linear relation between the conversion, which was defined as percentage of isobutene reacted, and the weight of catalyst; (ii) the methacrolein yield, which was defined as the percentage of isobutene converted to methacrolein, could be measurable for most of the samples studied. Using M^{I}_{50}, we found that the linearity between the conversion and catalyst weight could be assured when the conversion did not exceed 40%. This is the case for most samples when using 800 mg of catalyst (height of catalytic bed was 1 cm).

However, for some samples, e.g., M^{I}_{100} and M^{I}_{85}, such conditions would give rise to a conversion higher than 40% at high temperatures. Another risk in such conditions could be that the oxygen supply would become insufficient. For these samples, 400 mg of catalyst was used. For comparison purposes the results obtained are presented in the same scale as those measured at 800 mg, by simply multiplying isobutene conversion and methacrolein yield by a factor of 2.

In some tests, the partial pressure of oxygen was varied. Methacrolein selectivity was calculated as the ratio of yield over conversion. For each run, the catalyst was heated under the flow of the reaction mixture (N_2 + O_2 + isobutene) to the desired reaction temperature. Unless stated otherwise, the catalytic behavior of the sample was stable during the measurements. The reported results correspond to measurements made 1 h after the reaction temperature had been reached.

RESULTS

Physico-chemical Characterization

XRD. Only the results obtained with the more sensitive Siemens D-500 equipment are reported here. The same conclusion can be reached with the other diffractometer.

Figures 1a and 1b present the X-ray diffraction spectra for SnO_2(I)–Sb_2O_4 and SnO_2(II)–Sb_2O_4 systems, respectively. It can be observed that only the crystallographic phases characteristic of the pure oxides are observed in the mechanical mixtures. The only difference between the two figures is that the crystallinity of SnO_2(II) is better than SnO_2(I). Within the limit of detection of the diffractometer used, no new peak or shift of the peak position is observed. Compared to fresh samples, no difference is observed for the samples after the test.

BET. BET surface areas of pure oxides and mechanical mixtures (in the case of SnO_2(I)–Sb_2O_4) are reported in Table 2, for both fresh and used samples. Within the precision limit of the BET method, the surface

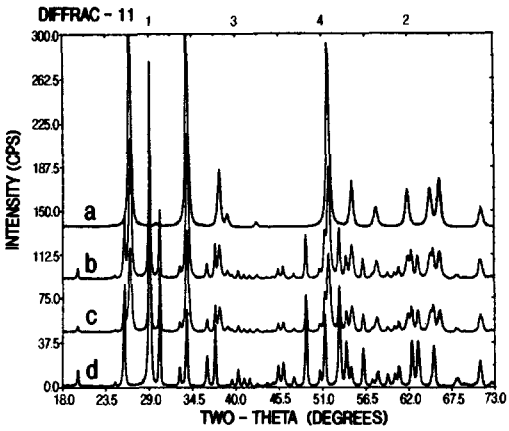

FIG. 1a. X-ray diffraction spectra for the SnO_2(I) + Sb_2O_4 system, (a) SnO_2(I), (b) M^{I}_{50} before reaction, (c) M^{I}_{50} after reaction, and (d) Sb_2O_4.

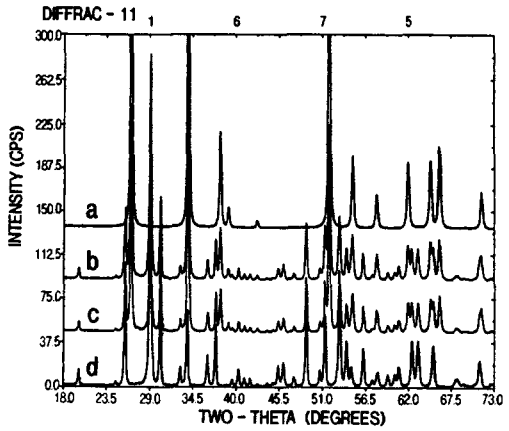

FIG. 1b. X-ray diffraction spectra for the SnO_2(II) + Sb_2O_4 system, (a) SnO_2(II), (b) M^{II}_{50} before reaction, (c) M^{II}_{50} after reaction, and (d) Sb_2O_4.

area of the mixture is the sum of those of the pure oxides for fresh samples. After catalytic reaction, the surface area of Sb_2O_4 was not changed, while a small increase was observed for pure SnO_2(I) and mechanical mixtures. In comparison with pure SnO_2, the increase of this surface area after reaction is smaller for mechanical mixtures, depending on the concentration of Sb_2O_4; i.e., the smaller the increase of the surface area, the higher the concentration of Sb_2O_4. After the samples were calcined in air at 400°C for 20 h, their BET surface areas regained their original values. This indicates that the increase of surface area is due to a deposit, and not to the change of the surface areas of the oxides. We demonstrate in the discussion that this change is due to the deposition of carbon (coke).

TABLE 2

BET Surface Areas for SnO_2(I)—Sb_2O_4 System ($m^2\ g^{-1}$)

Sample	M^{I}_{100}	M^{I}_{70}	M^{I}_{50}	M^{I}_{0}
Fresh sample	12.6	10.5	8.6	1.9
Used sample	17.7	11.3	9.2	2.0
Used sample calcined at 400°C, 20 h	11.9	10.1	8.5	1.9

^{119}Sn Mössbauer spectroscopy. The SnO_2(I)–Sb_2O_4 system was studied. The mechanical mixtures have almost the same IS and QS values as pure SnO_2 (IS $\approx \pm 0.02$ mm/s, QS $\approx$ 0.55 mm/s), even when they have worked catalytically. No reduction of SnO_2 was observed.

In the ordinary mixtures we prepared, a small change occurring to the SnO_2 particles as a consequence of their contact with Sb_2O_4 might remain undetected, because the corresponding signal would be diluted by the one coming from the portion of particles not in contact with Sb_2O_4. In order to investigate that portion, we designed a special experiment. SnO_2 50% by weight, with a particle size of 250–300 μm was mixed mechanically with 50% of Sb_2O_4 with a particle size of 500–800 μm. The mixture thus prepared was tested in the reaction and the two oxides were then separated by sieving. The SnO_2 particles that remained attached to Sb_2O_4 after sieving should be those suffering most from the contact or contamination if any. Both samples were subjected to Mössbauer measurement. For SnO_2 remaining attached to Sb_2O_4, the accumulation time is much longer than that for the other samples. No new signal appeared and only SnO_2 was observed.

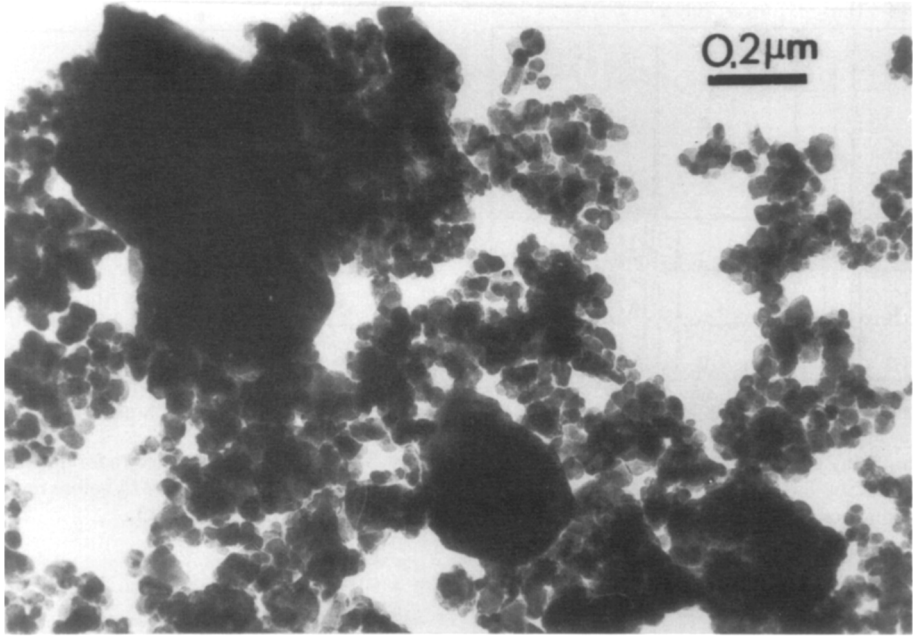

FIG. 2. CTEM micrograph for M^{I}_{50}.

ESR. No ESR signal with $g = 1.8733$ was observed in pure oxides or mechanical mixtures. This conclusion was also valid for all samples after having been used catalytically.

Electron Microscopy. Figure 2 shows a CTEM picture of mechanical mixture M^{I}_{50}, which can give an overview of the arrangement of the two oxides. The larger particles are Sb_2O_4, as identified by analytical electron microscopy. The smaller particles correspond to SnO_2. This difference in particle sizes corresponds to the BET results. Compared to the pure oxides, the particle sizes of SnO_2 and Sb_2O_4 are not modified after preparation of the mixture. This is also consistent with the BET surface area results (Table 2). The picture shows that the Sb_2O_4 crystallites are surrounded by SnO_2 particles. Some SnO_2 particles remain isolated.

The surface morphologies of both particles are shown in a SEM picture (Fig. 3) for the same sample. The surface of Sb_2O_4 is relatively smooth, while that of SnO_2 is irregular (these are actually aggregates).

Figure 4 shows two AEM spectra that were taken respectively from SnO_2 and Sb_2O_4 particles in M^{I}_{50}. Only the signals of the pure oxides were obtained. This indicates that within the experimental precision (contamination exceeding 1% at.), no contamination of one oxide by the other is detected.

The same conclusion is valid for the samples after having been used catalytically: these particles have morphologies similar to those of the fresh samples and no mutual contamination is detected.

XPS. The peaks do not change their shape, and binding energy values of $Sn_{3d_{5/2}}$, $Sn_{3d_{3/2}}$, $Sb_{3d_{5/2}}$, and $Sb_{3_{3/2}}$ are identical to ± 0.2 eV in all samples (before and after catalytic reaction) and correspond to those of pure SnO_2 and Sb_2O_4.

Figures 5a and 5b present the relative XPS concentrations (C_{sn}/C_{Si}, C_{Sb}/C_{Si}) as a function of the bulk atomic ratio Sn/(Sn + Sb) for SnO_2(I)–Sb_2O_4. For comparison, we report the Sn/(Sn + Sb) values deduced from XPS and those calculated theoretically (bulk

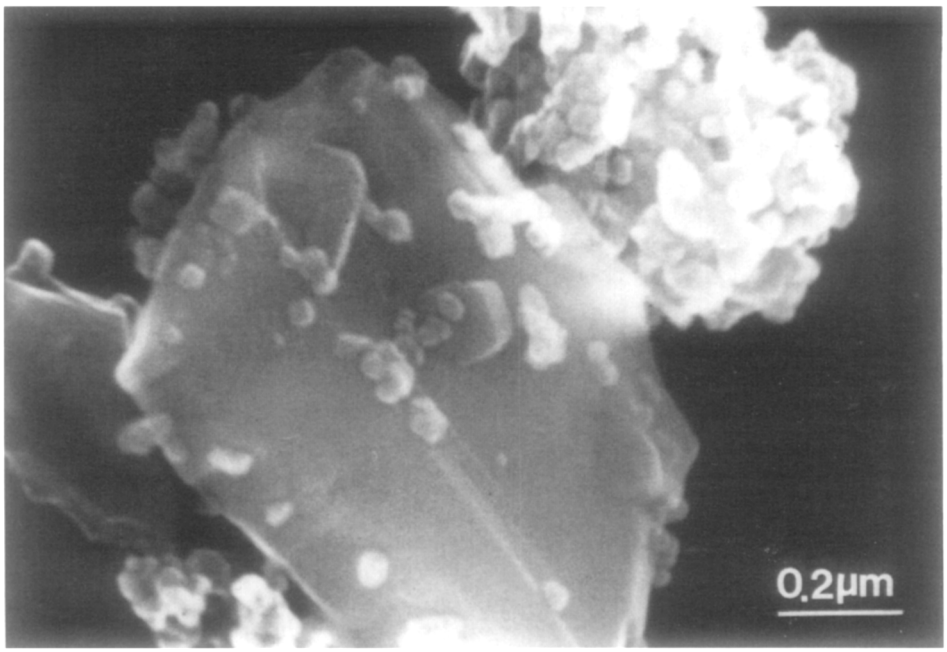

FIG. 3. SEM micrograph for M^{1}_{50}.

values) for these samples in Table 3. The following can be observed.

(i) As expected, the surface composition measured by XPS is different from that of the bulk for the fresh mixtures; i.e., we observe a relative enhancement of the signal of Sn.

(ii) With respect to fresh samples, the Sb XPS intensity remains almost constant after catalytic reaction while that of Sn decreases greatly. It follows that the Sn/(Sn + Sb) ratios determined by XPS decrease after the catalytic test (Table 3). However, this decrease is lower when Sb_2O_4 is present and the magnitude of this diminution depends on the quantity of the latter, namely the greater the quantity of Sb_2O_4, the smaller this decrease. In addition, we observe a great increase of C_{1s} intensity for used samples.

(iii) For used samples calcined in air at 400°C for 20 h, the Sn XPS intensity increases greatly and almost reaches its initial value. It follows that the Sn/(Sn + Sb) ratios almost regain their values before the catalytic test.

(iv) In comparison with the SnO_2(I)–Sb_2O_4 system, the SnO_2(II)–Sb_2O_4 mechanical mixture (last three lines at the bottom of Table 3) shows a smaller difference between the surface composition measured by XPS and bulk; i.e., we observe a smaller enhancement of the Sn signal. The other observations are similar, namely that the Sn/(Sn + Sb) ratio by XPS decreases after reaction and regains its initial value when the sample is calcined.

Catalytic Activity

The results concerning the catalytic properties of the SnO_2(I)–Sb_2O_4 mechanical mixtures are given in Figs. 6a, 6b, and 6c (the points represented by dotted lines correspond to results obtained using 400 mg of catalyst). They present, respectively, the variation of the overall conversion of isobutene, methacrolein yield, and selectivity as a function of mass ratio R_m, at 380, 400, and

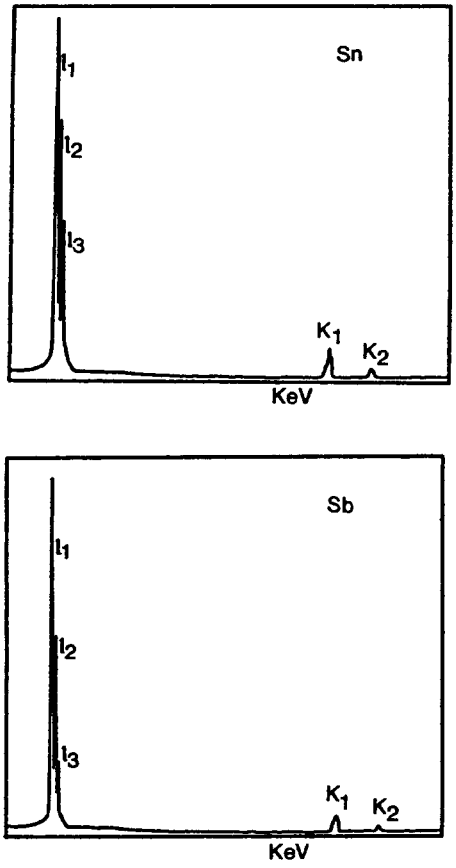

FIG. 4. Analytical microanalysis spectra for M^1_{50}, (a) taken from SnO_2(I) particle, (b) taken from Sb_2O_4 particle.

420°C. Pure Sb_2O_4 is inactive: no methacrolein, CO, or CO_2 was detected in our experiments. Pure SnO_2(I), however, is very active, but its selectivity is very poor. It transforms isobutene mostly to CO and CO_2. When SnO_2(I) is mixed mechanically with Sb_2O_4, however, the catalytic behavior is dramatically changed. The conversions of the mechanical mixtures are lower compared to the sum of those that would be observed with quantities of the isolated substances equal to those present in the mixture. This is true at low temperatures, i.e., 380 and 400°C; the conversion at 420°C increases almost linearly with SnO_2(I) content. The methacrolein yields (Fig. 6b)

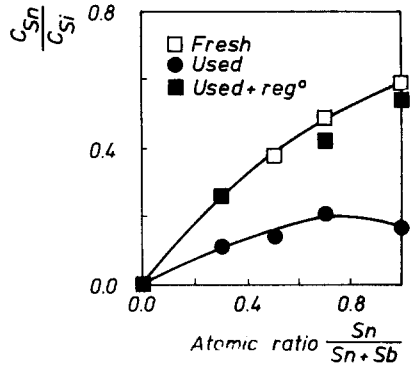

FIG. 5a. C_{Sn}/C_{Si} as a function of atomic ratio Sn/(Sn + Sb) for SnO_2(I) + Sb_2O_4 system.

measured with the mechanical mixtures, however, are much higher than those of the pure oxides; a strong synergy exists between Sb_2O_4 and SnO_2(I). All three curves pass through a maximum at a value of R_m near 0.5. Another manner of presenting the synergistic effect is to plot selectivity vs catalyst composition (Fig. 6c). With this representation, the maximum is located at R_m = 0.5 for low temperatures and it shifts to a smaller mass ratio when the temperature increases.

Similarly, the catalytic activity results for SnO_2(II)–Sb_2O_4 are reported in Figs. 7a, 7b, and 7c. It can be observed that the catalytic activity of this system is lower than that of

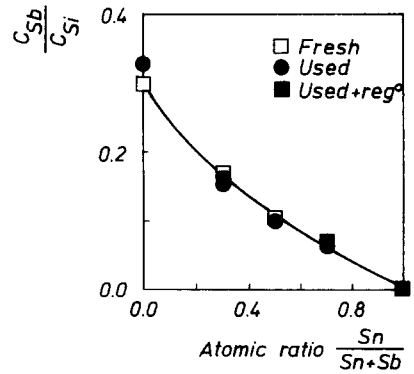

FIG. 5b. C_{Sb}/C_{Si} as a function of atomic ratio, Sn/(Sn + Sb) for SnO_2(I) + Sb_2O_4 system.

TABLE 3

Comparison of Sn/(Sn + Sb) Values Determined by XPS with Values by Bulk Analysis

Samples	Sn/(Sn + Sb) by XPS	Sn/(Sn + Sb) in bulk
M^{I}_{70}	0.871	0.704
M^{I}_{70} (after test)	0.749	
M^{I}_{70} (after test + reg.[a])	0.859	
M^{I}_{50}	0.785	0.505
M^{I}_{50} (after test)	0.590	
M^{I}_{30}	0.611	0.304
M^{I}_{30} (after test)	0.429	
M^{I}_{30} (after test + reg.[a])	0.616	
M^{II}_{50}	0.580	0.505
M^{II}_{50} (after test)	0.488	
M^{II}_{50} (after test + reg.[a])	0.560	

[a] Regeneration refers to the calcination of the sample at 400°C for 20 h.

the former. A conspicuous synergy is also observed for the methacrolein yield (Fig. 7b) and selectivity (Fig. 7c). However, the overall conversion of isobutene, especially at higher temperatures (420°C), varies almost linearly with the SnO_2 content. Compared with the first system, an important difference is observed, namely that the maxima of synergistic curves both for yield and for selectivity are observed around R_m = 0.75, instead of 0.5.

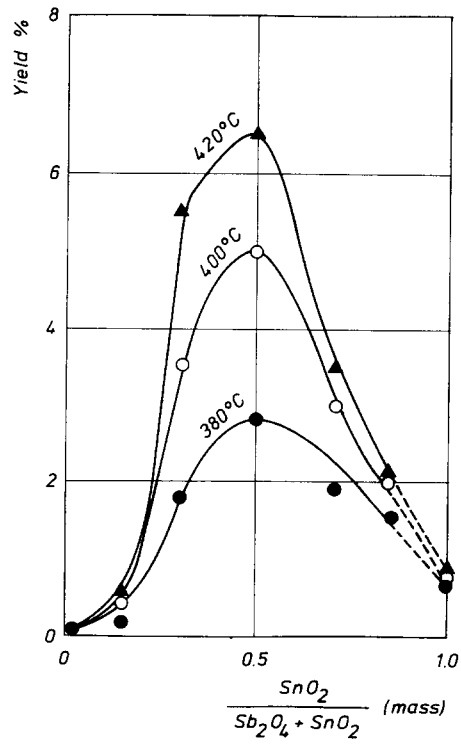

FIG. 6b. Methacrolein yield as function of R_m for SnO_2(I) + Sb_2O_4 mixtures.

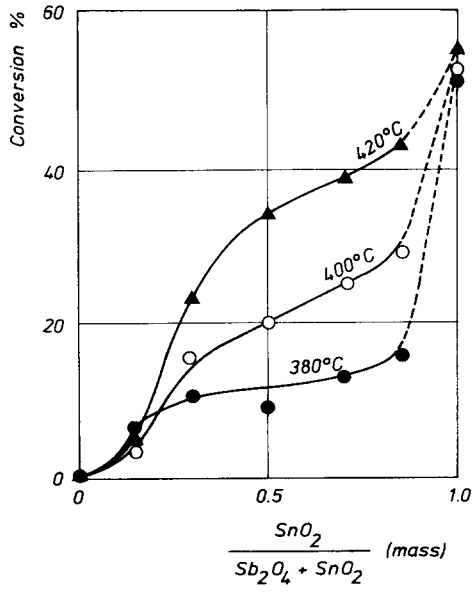

FIG. 6a. Isobutene conversion as a function of R_m for SnO_2(I) + Sb_2O_4 mixtures.

A second series of results concerns the role of oxygen. Figures 8a and 8b present, respectively, the variations of the overall conversion and methacrolein selectivity as functions of the oxygen/isobutene molar ratio for pure SnO_2(I) and mechanical mixtures M^{I}_{25}, M^{I}_{50}, and M^{I}_{75}. The overall conversion increases with the increase of oxygen concentration for all four samples (Fig. 8a). However, the increase for pure SnO_2(I) is more rapid than that for the mechanical mixture and the lower the concentration of Sb_2O_4 in the mechanical mixture, the steeper the increase of conversion.

The methacrolein selectivity for pure SnO_2(I) decreases toward zero when the oxygen concentration increases. On the contrary, for the mixtures, it increases progres-

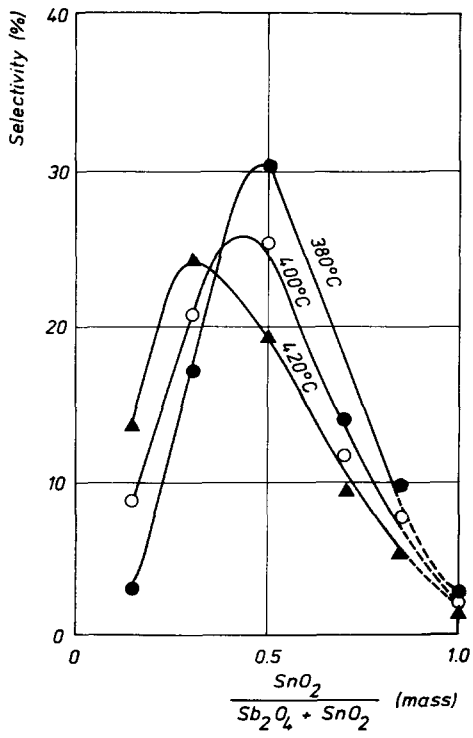

FIG. 6c. Methacrolein selectivity as a function of R_m for SnO_2(I) + Sb_2O_4 mixtures.

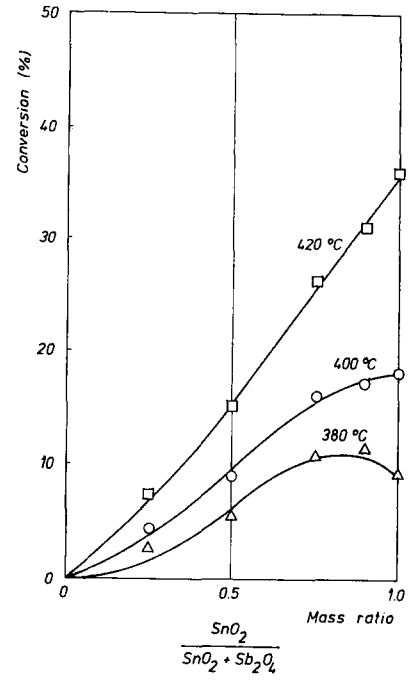

FIG. 7a. Isobutene conversion as a function of R_m for SnO_2(II) + Sb_2O_4 mixtures.

sively when little O_2 is present and then remains constant when the oxygen/isobutene ratio goes beyond a certain value (oxygen/isobutene $\approx$ 2 for M^I_{50}). It is interesting to note that the oxygen/isobutene ratio value, after which the selectivity remains constant, depends on the concentration of Sb_2O_4 in the mechanical mixtures (1.5, 2.0, and 3.5 for M^I_{25}, M^I_{50}, and M^I_{75}, respectively).

DISCUSSION

The above activity results show that SnO_2 and Sb_2O_4 work synergistically in the selective oxidation of isobutene to methacrolein, as did MoO_3–Sb_2O_4 (*2*). The cooperation between the two oxides is easily seen if we compare the results of M^I_{100} and M^I_{50}. For the same quantity of SnO_2(I) (400 mg), at 420°C, the conversion of M^I_{50} is only slightly higher than that of M^I_{100} (34% for M^I_{50} while

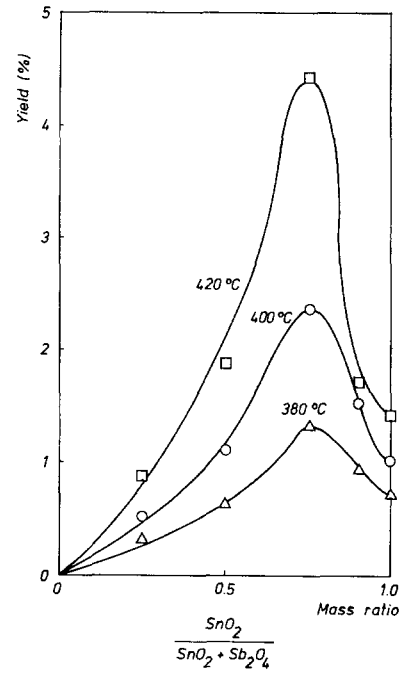

FIG. 7b. Methacrolein yield as a function of R_m for SnO_2(II) + Sb_2O_4 mixtures.

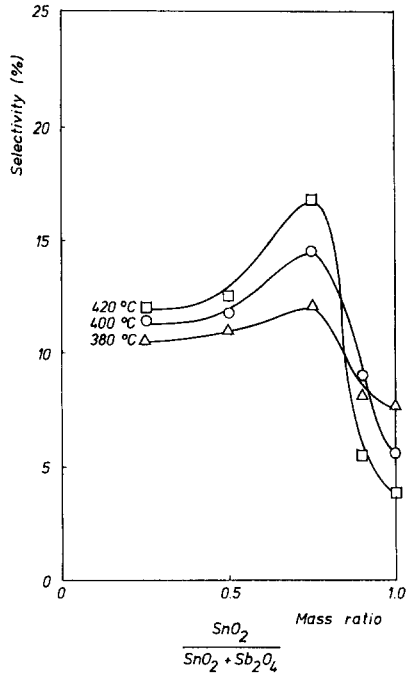

FIG. 7c. Methacrolein selectivity as a function of R_m for SnO_2(II) + Sb_2O_4 mixtures.

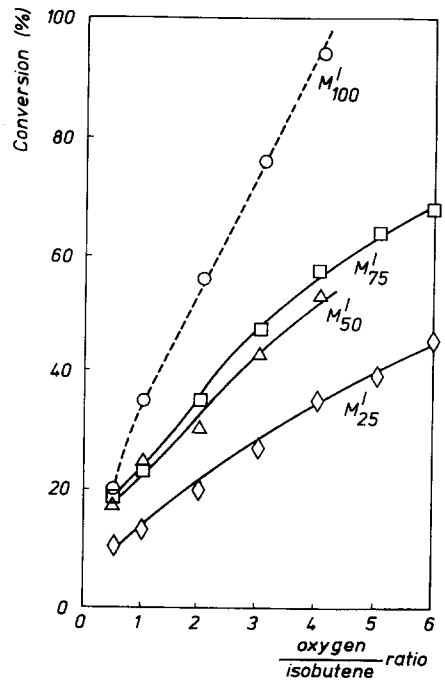

FIG. 8a. Isobutene conversion as a function of partial pressure of oxygen at 400°C for M^I_{100}, M^I_{75}, M^I_{50}, and M^I_{25}, respectively.

28% for M^I_{100}), but the selectivity of the former is at least 10 times greater than that of the latter. Consequently, the methacrolein yield of the former is 10 times greater than that of the latter. This comparison shows clearly that Sb_2O_4, although inactive when alone, improves strongly the selectivity of SnO_2(I). We mentioned in the Introduction that the synergy between two oxide phases can be explained by at least five mechanisms, depending on the interaction taking place between the two phases. In this discussion, we therefore examine the structure of the catalysts first, as characterized by the various techniques we used, then discuss the possible mechanisms involved, and finally give an interpretation of the results obtained.

1. *Physico-chemical Characterization*

1.1. Contamination (deposition) of coke. One surprising result observed in our experiment is that the BET surface area increases,

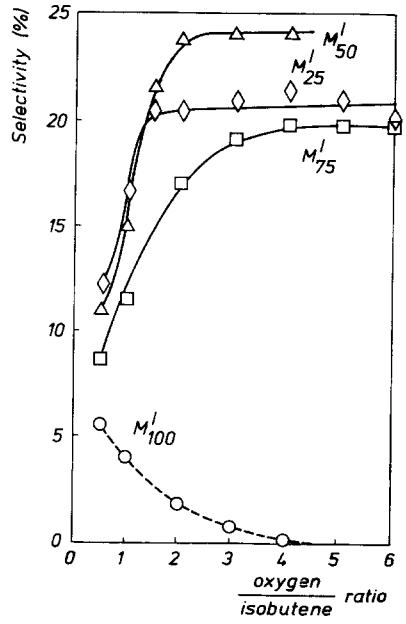

FIG. 8b. Methacrolein selectivity as a function of partial pressure of oxygen at 400°C for M^I_{100}, M^I_{75}, M^I_{50}, and M^I_{25}, respectively.

while the Sn XPS intensity decreases for pure SnO_2 and mechanical mixtures after reaction. However, after the samples have been calcined in air at 400°C for 20 h, the surface area and Sn XPS intensity almost regain the initial values observed for fresh samples. This suggests that the change of either surface area or Sn XPS intensity during catalytic reaction is due to a deposit. The fact that the samples become slightly black and that the C_{1s} XPS intensity increases greatly after reaction, especially for pure SnO_2, indicates that the deposit is a carbonaceous residue (coke). In addition, only a diminution of Sn XPS intensity is observed (not that of Sb); this indicates that the deposition of carbon takes place selectively on SnO_2.

We did not measure the exact amount of coke deposited on our samples. It is interesting to note that in the MoO_3–Sb_2O_4 mechanical mixtures, the carbon deposit can reach about 3% of the total weight of catalyst after the latter has been subjected to the dehydration of *N*-ethyl formamide in the absence of oxygen for 8 h (*29*). In our case, the quantity of coke might not be as high as that observed in the above case because gaseous oxygen is present.

Another interesting observation is that the change of surface area and Sn XPS intensity diminutions during reaction are smaller when Sb_2O_4 is present, and this effect increases with the quantity of the latter in the mixture. This indicates that the action of Sb_2O_4 protects the SnO_2 from coke deposition. The same conclusion had been obtained by the quantitative analysis of carbon deposit for the MoO_3–Sb_2O_4 system (*29*). This can be related to the ability of Sb_2O_4 to produce spillover oxygen, as discussed below.

1.2. Absence of new phase (or solid solution) formation. X-ray diffraction measurement, within the experimental precision, does not indicate the formation of any new phase by reaction between SnO_2 and Sb_2O_4 in the mechanical mixtures, even when they have been used for catalysis. According to the literature, the formation of a solid solution rather than of a new phase should be taken into account for Sn–Sb oxide catalysts. For this reason, we paid great attention to the displacement of the X-ray lines. The fact that no shift in the line positions was detected for the fresh and used samples suggests that no solid solution, such as Sb^{5+} dissolved in the SnO_2 lattice, as proposed in the literature, is formed either during preparation of the mixture or catalytic reaction. This conclusion is further confirmed by the results obtained with ^{119}Sn Mössbauer spectroscopy. However, it should be recognized that X-ray diffraction and Mössbauer spectroscopy are mass techniques and they therefore lack sufficient sensitivity to detect the possible formation of a small amount of a new phase or solid solution taking place at the interface (contact) between two oxides. Nevertheless, the specially designed Mössbauer experiment, in which the SnO_2 resting on the surface of Sb_2O_4 (and presumably having suffered most from the contact with the latter) was analyzed, may be considered as a more valuable approach to investigate the interfacial interaction between two oxides. Even in that case, no indication of solid solution formation is observed. Furthermore, ESR is very sensitive, but even with this technique, we cannot detect the signal characteristic of the formation of solid solution. The results obtained from these three techniques lead us to conclude that within the detection limits of these techniques, no new phase is produced and no solid solution is formed in our mechanical mixtures.

1.3. Absence of mutual surface contamination and monolayer formation. Analytical electron microanalysis shows that, within the sensitivity of the technique, only pure oxides are observed in our fresh and used mechanical mixtures. This suggests that no mutual contamination (by isolated atoms or in the form of monolayers) between two oxides takes place during the preparation of the mixture or catalytic reaction. However, it must be remembered that the overlap of the strong lines of Sn and Sb decreases the

sensitivity for detecting a possible contamination of SnO_2 surface by Sb.

The XPS results are more complicated. We observe a difference between the surface composition as measured by XPS and that of bulk for fresh SnO_2(I)–Sb_2O_4 mechanical mixtures; i.e., the XPS signals are more intense for Sn. As mentioned in the Experimental part, this can be explained by two possibilities: (i) the difference in particle size between SnO_2(I) and Sb_2O_4 and (ii) a possible surface contamination of Sb_2O_4 by Sn. The fact that, according to expectations, the difference is less in the case of SnO_2(II)–Sb_2O_4 mixtures (the surface of SnO_2(II) is 5.4 $m^2\ g^{-1}$ while that of SnO_2(I) is 12.6 $m^2\ g^{-1}$) leads us to attribute the increase of the Sn signal measured by XPS to the first possibility. However, in principle, the other explanation cannot be completely discarded. The diminution of the Sn XPS intensity after reaction has been explained by the deposition of coke during reaction. Therefore, if the influence of the coke deposition is taken into account (namely thanks to measurements after calcination), the Sn/(Sn + Sb) ratios remain practically equal for fresh and used mixtures. This indicates that, within the detecting limits of XPS, no mutual contamination between the two oxides takes place during the catalytic reaction, thus confirming the AEM results. As the method of preparation makes a contamination very unlikely (Sb_2O_4 or SnO_2 are not soluble in *n*-pentane), this confirms the view that the phases remain exempt from mutual contamination.

In conclusion, the joint use of all techniques applied in this study support the conclusion that, as in the MoO_3–Sb_2O_4 system, the mechanical mixtures of SnO_2 and Sb_2O_4 are constituted of two *separate, noncontaminated* oxide phases. This conclusion is further strongly confirmed by the results to be presented in the second part of this series of publications concerning the impregnated catalysts (*26*). In the corresponding experiments, the pure oxides (SnO_2 or Sb_2O_4) are impregnated with the other ion (Sb ions for SnO_2 and Sn ions for Sb_2O_4), in order to favor as much as possible a mutual surface contamination if it can take place. The characterization results of this other work show that the impregnated ions, instead of combining with their "support," tend to segregate to form two-phase catalysts during catalytic reaction. At the temperatures used, thermodynamics indeed favor decontamination. References concerning the preparation methods resulting in solid solutions usually involve coprecipitation and sometimes calcination of SnO_2 and Sb_2O_3 or Sb_2O_5 at extremely high temperature (±1000°C) (*30*). It is evident that all these preparation conditions are far different from those used in our experiment.

2. *Mechanism*

The above discussion shows that there is a complete lack of experimental evidence for the first three possibilities mentioned in the Introduction to explain the observed synergy, namely formation of a mixed oxide or a solid solution, surface contamination of one oxide by the other, and monolayer formation. Let us now look at the fourth possibility, a bifunctional mechanism.

The bifunctional mechanism assumes that a reactant is first adsorbed on one phase and transformed to an intermediate. This intermediate will then diffuse or migrate to the second phase, where it will react further with another reactant and will be converted into a product, which will finally desorb. If this mechanism operated in our system, we should thus accept that an intermediate such as, e.g., $[CH_2\text{---}C(CH_3)\text{---}CH_2]$ could desorb from one phase and readsorb for further reaction on the other one. However, this interpretation would raise several difficulties. First, the only intermediate for olefin oxidation evoked in the literature is the allylic species. The literature does not invoke its desorption. Theoretical calculations show the allylic species to be extremely strongly adsorbed (*31*). Second, the assumption that part of the reaction takes place on Sb_2O_4 contradicts the evidence

that Sb_2O_4 is almost absolutely inert. Conversely, the fact that SnO_2 reacts, even alone, suggests that it is involved both in the adsorption and reaction steps.

When two noncontaminated phases cooperate in a catalytic reaction and a bifunctional mechanism cannot be assumed, some surface migration (or diffusion) must necessarily take place. Migration of the adsorbed allylic species between two different faces of bismuth molybdate has been assumed in a few publications (*32*). If we contemplated the migration of a semi-reacted species (from one type of catalytic or adsorption center on one phase to another type on the other), this species would be composed of numerous atoms (11), taking an allylic species as a candidate for migration. The migration of an oxygen species, presumably composed of one atom (at most 2), is far easier because it is much smaller. Entropic consideration taking into account the multiple configurations of adsorption of a molecule with several atoms would suggest still more dramatic differences in favor of the oxygen species. Migration of oxygen could have explained the results leading to the hypothesis of migration of the allylic species between crystallographic faces just mentioned, and this would have been consistent with all the concepts developed in allylic oxidation.

It thus seems more logical to retain this last possibility, namely the migration of oxygen species. As a matter of fact, the migration of oxygen species and its effect have been experimentally indicated on some metal catalysts (*33–35*) and recently we have proven the migration of oxygen species from Sb_2O_4 to MoO_3 using ^{18}O (*36*).

Our discussion thus leads us to conclude that an oxygen species is formed on one phase and migrates over to the second one. If we accept this conclusion, we must consider two possibilities: (i) the mobile oxygen species is used as a reactant, and (ii) the mobile oxygen species is used as a "controlling" species to improve the catalytic properties of the second phase.

Before analyzing each hypothesis in detail, it is convenient to define a phase that produces mobile oxygen, as a donor D, and the phase that accepts mobile oxygen as an acceptor A. In our case, A is obviously SnO_2, which carries the active centers. The role of Sb_2O_4, inactive in the reaction, is, by necessity, limited to that of donor.

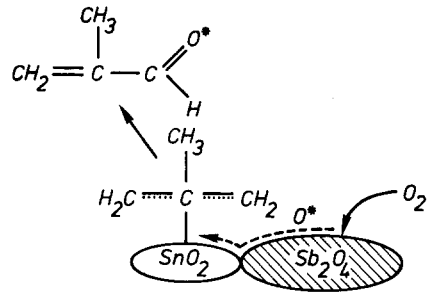

SCHEME 4. Spillover oxygen used as a reactant.

(*a*) *Spillover oxygen used as a reactant.* This mechanism has been proven experimentally for the MoO_3–Sb_2O_4 system in the oxidation of propylene in the absence of gaseous O_2 (*36*). The schematic representation of this mechanism, as it would be transformed to the SnO_2–Sb_2O_4 system, is given in Scheme 4. The oxygen species O* emitted by Sb_2O_4 migrates to the surface of SnO_2, where it reacts either directly with adsorbed isobutene or indirectly, i.e. the oxygen species O* would firstly occupy lattice vacancies on SnO_2 and then become incorporated into the isobutene intermediate (O* would be used as a lattice oxygen, according to the accepted terminology in allylic oxidation). Accepting a detailed mechanism proposed in Ref. (*1*), SnO_2, in this case, might be considered to function as Mo does in bismuth molybdates (chemisorption of isobutene and insertion of oxygen) while Sb_2O_4 functions like the Bi–O–Bi site (chemisorption, reduction, and dissociation of molecular oxygen).

The assumption that spillover oxygen would work as a reactant cannot be absolutely excluded. However, if we adopt this interpretation, several difficulties appear. (i) If this is the case, the main role of Sb_2O_4

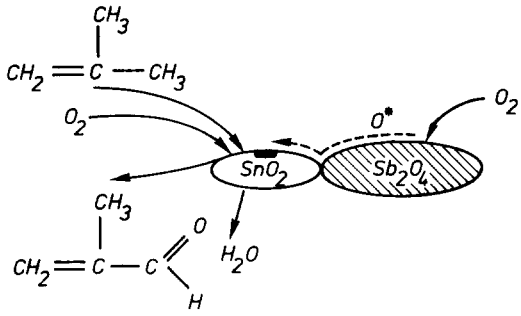

SCHEME 5. Spillover oxygen is used as an activating species for creating or regenerating catalytic sites.

would be to provide more reactant, namely to increase the overall conversion of isobutene by providing more oxygen rather than promoting methacrolein *selectivity*. This is contrary to our results, namely that the addition of Sb_2O_4 to SnO_2 has almost no effect on the overall conversion but increases considerably the methacrolein selectivity. An effect of Sb_2O_4 on the selectivity to selective oxidation products has also been observed in several other two-phase systems (*2, 5*). (ii) The production of spillover species is usually not a very efficient process (*37*). Presumably, a very large amount of Sb_2O_4 would be needed for providing a noticeable effect and, relative to the amount of SnO_2 present, the largest methacrolein yield would be expected when Sb_2O_4 would be in large excess because, under these conditions, the surface of SnO_2 could be "flooded" with the largest quantity of active oxygen species. This is not in agreement with our results that the maximum yield is always observed at moderate mass ratio values (near to 0.5). This is remarkable, as contacts between particles in mechanical mixtures are neither very numerous nor very intimate.

(*b*) *Spillover oxygen used as a "controlling" species*. This corresponds to the remote control mechanism as described in the Introduction. It is simply presented in Scheme 5. By analogy with the MoO_3–Sb_2O_4 system, the fact that pure SnO_2 is very active suggests that SnO_2, like MoO_3, carries the necessary functions for oxidation. Isobutene adsorbs on SnO_2 and is subsequently transformed to oxidation products. This process is accompanied by the reduction of the catalytic surface sites on SnO_2, which are thereafter reoxidized by oxygen (catalytic cycle). Sb_2O_4, on the other hand, produces spillover oxygen O*, which migrates onto the surface of SnO_2, where it reacts to create and regenerate the selective catalytic sites. In this way, the number of selective catalytic sites depends on the quantity of spillover oxygen available on the surface of SnO_2. This is fully in agreement with our results and, especially, with the spectacular change in selectivity, namely the proportion of selective sites as a function of composition. For convenience, we have redrafted the two methacrolein yield vs R_m curves at 400°C in Fig. 9 for SnO_2(I)—Sb_2O_4 and SnO_2(II)—Sb_2O_4 systems, respectively. In the context of the remote control mechanism, the fact that the maximum yield for SnO_2(I)—Sb_2O_4 is observed at R_m near 0.5 (curve 1) can be ex-

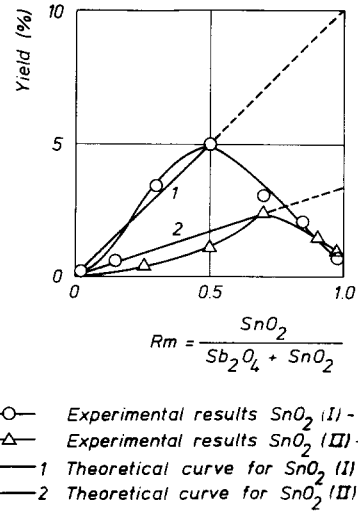

FIG. 9. Comparison between the methacrolein yield observed experimentally and those predicted theoretically based on the remote control mechanism for two series of SnO_2 + Sb_2O_4 mixtures.

plained by saying that at this point all SnO_2(I) can be most efficiently activated by spillover oxygen, i.e., that 2 m^2 Sb_2O_4 (1 g) can activate 12.6 m^2 SnO_2(I) (1 g). The decrease of the yield on the left side is due to the decrease of the quantity of SnO_2 (or the maximum number of catalytic sites available for activation). The decrease on the right side is caused by the fact that the quantity of Sb_2O_4 present becomes insufficient (or that too little spillover oxygen is produced) for maintaining the selectivity of the sites. If we follow this reasoning, we should observe a curve composed of a straight line on the left, and a curve possibly more complicated on the right, intersecting at R_m near 0.5. The dotted line represents the results that would be observed if all SnO_2 could be activated as in the case of $R_m = 0.5$.

Now, if we have 1 g SnO_2(II) (or 5.4 m^2 SnO_2) instead of SnO_2(I), we can easily estimate the amount of Sb_2O_4 necessary to activate it most efficiently. In other words, we can easily estimate the position of maximum yield for the SnO_2(II)—Sb_2O_4 system using the following formula: $2/12.6 = [(1 - R_m) \times 2]/[R_m \times 5.4]$. The result, $R_m = 0.7$, is very close to that observed experimentally (curve 2 in Fig. 9). In the same way, we can draw the theoretical curve for this system. The comparison between the theoretical and experimental curves shows that the prediction of the remote control mechanism matches well the results obtained, not only with respect to the position but also of the maximum magnitude.

Without absolutely excluding some participation of spillover oxygen as reactant, we are thus led to conclude that the effects we observed are mainly due to a remote control effect. Therefore, in what follows, we interpret our results in detail within the context of this mechanism.

3. Interpretation of the Results on the Basis of the Remote Control Mechanism

3.1. Influence of mixture composition (R_m). The effect of R_m on the methacrolein yield has been clarified in the preceding paragraph. Now let us look at its influences on overall conversion and selectivity.

Account having been taken of possible perturbations due to near exhaustion of oxygen in certain experiments, the overall conversion is roughly proportional to the amount of SnO_2 present in the catalyst. The enhancement of the methacrolein yield takes place essentially thanks to the increase of its selectivity (Figs. 6 and 7). This indicates that the role of Sb_2O_4 is essentially to transform the nonselective sites on SnO_2 to selective ones, while not changing much the total catalytic site number. Sb_2O_4 renders SnO_2 more selective.

The selectivity curves as a function of mass ratio for the SnO_2(I)—Sb_2O_4 system (Fig. 6c) show that the selectivity maximum is also observed at mass ratio near 0.5. This seems surprising because, if there were no perturbation to the remote control mechanism, the selectivity would have increased continuously with the increase of Sb_2O_4/SnO_2, i.e., moving to the left. We have no strongly supported explanation for this fact. We may speculate that the effect might be related to the special characteristics of SnO_2. The curve corresponding to SnO_2 in Fig. 8b shows that this oxide tends to lose selectivity when the oxygen concentration increases and the selectivity becomes almost zero when the oxygen/isobutene ratio (in the absence of remote control) is in excess of 3. We may thus reason that, when Sb_2O_4 is in too large a proportion, too much spillover oxygen is present on the surface of SnO_2 and its surface becomes somehow "overoxidized" as it becomes in the presence of too high an oxygen concentration. The spillover oxygen O* is very likely the nucleophilic species O^{2-}. This follows logically the fact that the presence of Sb_2O_4 greatly improves the selectivity. This would be incompatible with the presence of electrophilic species on the surface. This explanation of the deleterious effect of too high an oxygen pressure may be easily understood if we accept the equation

$$2O^* (O^{2-}) + O_2 \rightarrow 4O^- \text{ (or } 2O_2^{2-}). \quad (3)$$

The implication of this equation is that too much spillover oxygen may cause the production of electrophilic species on the SnO_2 surface, which is detrimental to selectivity.

The question is, How does Sb_2O_4 make SnO_2 more selective? Usually when dealing with selective oxidation catalysts, one must pay much attention to the oxidation—reduction phenomenon taking place on the surface. It has usually been accepted that the optimal selectivity of the catalyst is found when the catalyst is in an optimal oxidation state. Therefore, it seems that the presence of Sb_2O_4 would keep SnO_2 in a "suitable" oxidation state. It is not easy to disentangle the various effects brought about by spillover oxygen.

The results of Figs. 6b and 7b show that spillover oxygen creates the selective sites for oxidation. However, the exact mechanism by which these selective sites are created is not easy to analyze. We have seen that some coke was deposited. This coke, presumably, can play a role in modifying the activity of catalytic sites, possibly impairing selectivity. It is impossible to separate the contribution of the creation and regeneration of active sites by spillover oxygen. However, the observed results lead us to make some speculation. Essentially, the role of spillover oxygen may be linked to the possibility of deep reduction of the SnO_2 surface, or of deposition of coke. We examine both possibilities.

In conformity with accepted mechanisms, the oxidation of isobutene on SnO_2 is accompanied by surface reduction of SnO_2. The reduced sites on SnO_2 should be reoxidized immediately, otherwise a reduced surface would be formed and selectivity would decrease. The activity results seem to indicate that SnO_2 suffers from more rapid reactivity with respect to molecular oxygen, or the reoxidation of reduced SnO_2 being rate-limiting. It has been demonstrated that the migration of lattice oxygen from the bulk of SnO_2 is very low compared to the consumption of oxygen on the surface (*38*). Lattice oxygen cannot compensate for a loss of oxygen on the surface. Therefore, the explanation for the increase of methacrolein selectivity is that the spillover oxygen (O*) emitted by Sb_2O_4 helps prevent the reduction of SnO_2, and consequently maintains the selectivity. A similar phenomenon, namely that the spillover oxygen protects pure $ZnFe_2O_4$ from deep reduction, even phase segregation, has been clearly demonstrated in the case of oxidative dehydrogenation of *n*-butene (*39*).

If the above explanation is correct, namely that an oxygen spillover species is at stake, one should observe similar effects in solid state reactions, e.g., an increase of the reoxidation rate of the active phase owing to the presence of a donor phase. This has indeed been proven for the MoO_3—Sb_2O_4 system by a specially designed experiment (*29*) in which the MoO_3 was prereduced with pure H_2; one portion of this reduced MoO_3 was mixed mechanically with Sb_2O_4 and the reoxidation of reduced MoO_3 was studied gravimetrically for both samples. Since the spillover is a reversible phenomenon, the inverse process should also take place: if the active phase is reduced, more rapid removal of oxygen from it would take place (e.g., MoO_3 or SnO_2) when the donor phase (Sb_2O_4) of spillover oxygen is present. This has been experimentally observed for both MoO_3—$BiPO_4$ (*20*) and MoO_3—Sb_2O_4 (*29*) systems.

The inhibition of deposition of carbon or elimination of this coke by spillover oxygen is clearly demonstrated in our case. The decrease of XPS Sn intensity is less important when Sb_2O_4 is present, the magnitude of this effect depending on the quantity of the latter in the mixtures. The logical explanation for these results is that the spillover oxygen produced by Sb_2O_4 can burn out either the precursors of coke, thus inhibiting the formation of carbonaceous deposits, or the coke itself, when it is formed more efficiently than gaseous (molecular) oxygen. In the same perspective, the larger diminution of Sn

XPS intensity for pure SnO_2 can easily be explained by the absence of spillover oxygen. The results do not give strong enough information for analyzing more in depth the role of spillover oxygen. In particular, deposition of coke might be a cause of deactivation (as it is for acidic sites in hydrogen-involving reactions); however, it might as well be a consequence of the loss of selectivity accompanying the reduction of the surface. Correspondingly, the role of spillover oxygen (O*) can be either to protect the selective sites against reduction or to burn the deposit of coke.

These possibilities are explained schematically as follows:

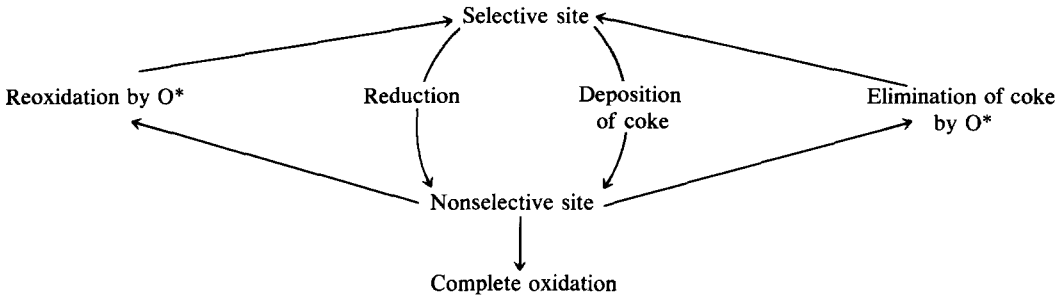

3.2. Reaction temperature. The effect of the reaction temperature on catalytic activity is quite different for pure SnO_2 and for the mechanical mixture. For pure SnO_2 or Sb_2O_4-poor mixture, increasing the reaction temperature rapidly increases total conversion and not the methacrolein yield (Figs. 6a, 6b, 7a, 7b). In other words, the increase of reaction temperature favors total oxidation to CO and CO_2. In the mechanical mixture, the effect of temperature must be more complex. First, as for pure SnO_2, an increase in reaction temperatures tends to favor total oxidation (or decrease the selectivity). Second, an increase in reaction temperatures also enhances the rate of migration of spillover oxygen, which is favorable for selectivity. The overall selectivity of the mechanical mixture depends on these two antagonistic processes. The fact that the selectivity increases with reaction temperature for the mechanical mixtures rich in Sb_2O_4 (left part of Fig. 6c) suggests that the second parameter plays a dominant role. On the contrary, for the mechanical mixtures rich in SnO_2 (right part in Fig. 6c), the first parameter dominates. This phenomenon has a corollary, namely the interesting shift from right to left of the selectivity maximum when reaction temperature increases. With the increase of temperature, SnO_2 becomes more and more active and also less selective. To arrive at a good selectivity, more Sb_2O_4 is necessary to "irrigate" with more spillover oxygen the surface of SnO_2. These effects are noticeable with the mixture containing SnO_2(I). They are still more conspicuous with SnO_2(II), which, because of its lower surface area, exerts a weaker effect.

3.3. Partial pressure of oxygen. The remote control mechanism demands the presence of spillover oxygen. The partial pressure of oxygen therefore necessarily influences the catalytic activity and selectivity in different ways when Sb_2O_4 is present or absent. This is clearly demonstrated in Figs. 8a and 8b.

For pure SnO_2, the increase of oxygen concentration quickly enhances total conversion, whereas the selectivity decreases. This means that the increase of oxygen concentration is unfavorable for selective oxidation. This may be explained by the increase in the formation of electrophilic

oxygen species (O_2^-, or O^-), as shown by Eq. (3). The presence of these electrophilic species on SnO_2 surface has been evidenced by ESR (*40*).

For the mechanical mixtures, however, two parameters must be taken into account. The first is the same as for pure SnO_2, namely that the increase of oxygen concentration is unfavorable for selectivity. The second is that the increase of oxygen concentration would favor the production of spillover oxygen, which is favorable for selectivity. The fact that the selectivity increases at low oxygen/isobutene ratios as oxygen concentration increases suggests that the second parameter plays a determining role. Similarly, the fact that the selectivity is independent of oxygen concentration at higher oxygen/isobutene ratios means that the influence of the two parameters is comparable.

Comparing the results of Fig. 8b corresponding to the three mechanical mixtures, some interesting points emerge. The mechanical mixture rich in Sb_2O_4 can arrive at "saturation" point earlier than that rich in SnO_2 (compare M^I_{25} and M^I_{75}). This again confirms the role of Sb_2O_4, namely the production of spillover oxygen. With more Sb_2O_4 present in the mechanical mixture, more spillover oxygen is available at the same oxygen concentration and consequently the saturation point is reached for a lower oxygen pressure.

According to Eq. (3), one may expect a decrease of selectivity at very high oxygen concentrations for the mechanical mixtures and this would occur more readily for M^I_{25} than for M^I_{75}. The last experimental points for M^I_{25} in Fig. 8b might be considered as an indication of this.

Summarizing, the remote control mechanism satisfactorily explains the results obtained with mechanical mixtures of SnO_2 and Sb_2O_4.

CONCLUSIONS

Our work has demonstrated several findings:

—The mechanical mixtures of SnO_2 and Sb_2O_4 exhibit a cooperation in selective oxidation of isobutene to methacrolein. The addition of Sb_2O_4 (inert when alone) to SnO_2 essentially improves the selectivity of the reaction to methacrolein, whereas it has almost no effect on overall conversion.

—The joint use of physico-chemical techniques such as XRD, ^{119}Sn Mössbauer spectroscopy, electron microscopy, AEM, XPS, and ESR for the characterization of fresh and used samples fails to give any evidence of the formation of a new compound (or solid solution) or mutual surface contamination between the oxides in the mechanical mixtures. Within the limits of sensitivity of the techniques used, the mechanical mixtures appear to be composed of two separate oxide phases.

—The possible mechanisms explaining the observed synergy have been discussed. The most plausible one is the remote control mechanism. The results obtained can all be satisfactorily explained taking the remote control mechanism as a basis.

ACKNOWLEDGMENTS

We gratefully thank the Université Catholique de Louvain, the Chinese Government for financial support of one of us (L. T. Weng), and the Service de Programmation de la Politique Scientifique for support of this research. We also thank Dr. J. Naud for some XRD measurements and Dr. T. Machej for fruitful discussions.

REFERENCES

1. Grasselli, R. K., and Burrington, J. D., *in* "Advances in Catalysis" (D. D. Eley, H. Pines, and P. B. Weisz, Eds.), Vol. 30, p. 133. Academic Press, San Diego, 1981.
2. (a) Ruiz, P., Zhou, B., Remy, M., Machej, T., Aoun, F., Doumain, B., and Delmon, B., *Catal. Today* **1**, 181 (1987). (b) Weng, L. T., Zhou, B., Yasse, B., Doumain, B., Ruiz, P., and Delmon, B., *in* "Proceedings, 9th International Congress on Catalysis, Calgary, 1988" (M. J. Phillips and M. Ternan, Eds.), Vol. 4, p. 1609. Chem. Institute of Canada, Ottawa, 1988.
3. Okamoto, Y., Hashimoto, T., Imanaka, T., and Teranishi, S., *Chem. Lett.* 1035 (1978).
4. Okamoto, Y., Oh-Hiraki, K., Imanaka, T., and Teranishi, S., *J. Catal.* **71**, 99 (1981).
5. Volta, J. C., Bussière, P., Coudurier, G., Herr-

mann, J. M., and Védrine, J. C., *Appl. Catal.* **16,** 315 (1985).
6. Wolfs, M. W. J., and Batist, Ph. A., *J. Catal.* **32,** 25 (1974).
7. Prasada Rao, T. S. R., and Krishnamurthy, K. R., *J. Catal.* **95,** 209 (1985).
8. Isaev, O. V., and Margolis, Ya., *in* "Preparation of Catalysts" (B. Delmon, P. A. Jacobs, and G. Poncelet, Eds.), p. 177. Elsevier, Amsterdam, 1976.
9. Ozkan, U. S., and Schrader, G. L., (a) *J. Catal.* **95,** 120 (1985); (b) *J. Catal.* **95,** 137 (1985).
10. Grzybowska, B., and Mazurkiewicz, A., *Bull. Acad. Polon. Sci.* **28,** 141 (1979).
11. Organowski, W., Hanuza, J., Jezowska-Trzebiatowska, B., and Wrzyszcz, J., *J. Catal.* **39,** 161 (1975).
12. Okamoto, Y., *J. Chem. Soc. Chem. Commun.,* 1018 (1981).
13. Kremenic, G., Fierro, J. L. G., and Cortes Corberan, V., "Acta. 8th Simposium Iberoamericano de Catalysis, LaRabida (Spain)," Vol. 1, p. 346. Malquisa, Madrid, 1982.
14. Grasselli, R. K., Brazdil, J. F., and Burrington, J. D., *J. Catal.* **79,** 104 (1983).
15. Teller, R. G., Brazdil, J. F., and Grasselli, R. K., *J. Chem. Soc. Faraday Trans. 1* **81,** 1693 (1985).
16. Yamazoe, N., Aso, I., Amamoto, T., and Seiyama, T., *in* "Proceedings, 6th International Congress on Catalysis, London, 1976" (G. C. Bond, P. B. Wells, and F. C. Tompkins, Eds.), p. 1239. The Chemical Society, London, 1977.
17. Carson, D., Coudurier, G., Forissier, M., and Védrine, J. C., *J. Chem. Soc. Faraday Trans. 1* **79,** 1921 (1983).
18. Wang, H. Q., Feng, L. P., Chen, Y. W., Miao, D. X., Cong, Q. Z., and Jiang, A. B., *Sci. Sin.* **12,** 1397 (1979).
19. Gibson, M. A., and Hightower, J. W., *J. Catal.* **41,** 431 (1976).
20. Tascon, J. M. D., Grange, P., and Delmon, B., *J. Catal.* **97,** 287 (1986).
21. Zhou, B., Ceckiewicz, S., and Delmon, B., *J. Phys. Chem.* **91,** 5061 (1987).
22. Roginskaya, Yu. E., Dulin, D. A., Strovea, S. S., Kul'kova, N. N., and Gel'bshtein, A. I., *Kinet. Katal.* **9,** 1143 (1968).
23. Berry, F. J., *in* "Advances in Catalysis" (D. D. Eley, H. Pines, and P. B. Weisz, Eds.), Vol. 30, p. 97. Academic Press, San Diego, 1981.
24. Pyke, D. R., Reid, R., and Tilley, R. J. D., *J. Chem. Soc. Faraday Trans. 1* **76,** 1174 (1980).
25. Kustova, G. N., Tarasova, D. V., Olen'kova, I. P., and Chumachenko, N. N., *Kinet. Katal.* **17,** 744 (1974).
26. Weng, L. T., Yasse, B., Ladrière, J., Ruiz, P., and Delmon, B., *J. Catal.* **132,** 343 (1991).
27. Berry, F. J., *Inorg. Chim. Acta.* **50,** 85 (1981).
28. Wagner, C. D., Davis, L. E., Zeller, M. V., Taylor, P. A., Raymond, R. H., and Gale, L. H., *Surf. Interface Anal.* **3,** 21 (1981).
29. Zhou, B., Ph.D. thesis, Université Catholique de Louvain, 1988.
30. Wakabayashi, K., Kamiya, Y., and Ohta, N., *Bull. Chem. Soc. Jpn.* **40,** 2172 (1967).
31. Haber, J., and Witko, M., *Acc. Chem. Res.* **14,** 1 (1981).
32. Brückman, K., Haber, J., and Wiltowski, T., *J. Catal.* **106,** 188 (1987).
33. Ekstrom, A., Batley, G. E., and Johnson, D. A., *J. Catal.* **34,** 106 (1974).
34. Ducame, V., and Védrine, J. C., *J. Chem. Soc. Faraday Trans. 1* **74,** 506 (1978).
35. Baumgarten, E., and Schuck, A., *Appl. Catal.* **37,** 247 (1988).
36. Weng, L. T., Duprez, D., Ruiz, P., and Delmon, B., *J. Mol. Catal.* **52,** 349 (1989).
37. Hodnett, B. K., and Delmon, B., *in* "Studies in Surface Science and Catalysis" (L. Červeny, Ed.), Vol. 27, p. 53. Elsevier, Amsterdam, 1985.
38. Fattore, V., Fuhrman, Z. A., Manara, G., and Notari, B., *J. Catal.* **37,** 215 (1975).
39. Qiu, F. Y., Weng, L. T., Sham, E., Ruiz, P., and Delmon, B., *Appl. Catal.* **51,** 235 (1989).
40. Cheng, S. C., *J. Vac. Sci. Technol.* **17,** 366 (1980).